JTEIN: Jurnal Teknik Elektro Indonesia
Vol. 4, No. 2, 2023
e-ISSN 2723-0589
DOI: https://doi.org/10.24036/jtein.v4i2.508
http://jtein.ppj.unp.ac.id

Renewable Energy Contribution Based on Microgrid Using Photovoltaic and Wind Turbine Scenario

Handoko Rusiana Iskandar*)1, Yusuf Irwin Deriantono2, Dede Furqon3, Naftalin Winanti4
1234Electrical Engineering Department, Faculty of Engineering, Universitas Jenderal Achmad Yani
*)Corresponding author, handoko.rusiana@lecture.unjani.ac.id

Abstrak

Bauran Energi Terbarukan di Indonesia memberikan alternatif energi selain energi sumber fosil yang konvensional. Sesuai dengan *Paris Agreement* indonesia memiliki komitmen kuat untuk peranan pemanfaatan energi baru tersebut. Makalah ini merupakan usulan desain arsitektur *microgrid* pembangkit listrik hibrida energi surya dan angin dengan konfigurasi terhubung jaringan PLN dengan pemodelan pembangkit skala mikro di Desa Ciheras, Kecamatan Cipatujah, Kabupaten Tasikmalaya, Jawa Barat. Arsitektur ini dimodelkan menjadi tiga skenario untuk mencari karakteristik desain yang paling optimal. Skenario pertama yaitu *Photovoltaic* (PV) 50% dan *Wind Turbine* (WT) 50%, skenario kedua yaitu PV 60% dan WT 40% serta skenario ketiga yaitu PV 70% dan WT 30%. Perbandingan hasil dari microgrid terhubung jaringan dilakukan menggunakan perangkat lunak pendukung yaitu HOMER Pro. Analisis performa dan kontribusi energi terbarukan dihasilkan dari berbagai skenario yang dibuat. Pemodelan, perhitungan, simulasi hingga analisis menunjukkan potensi produksi energi pada skenario pertama menghasilkan 25.655 kWh/tahun dengan Renewable Fraction sebesar 88,2%. Skenario kedua memiliki produksi energi sebesar 26.194 kWh/tahun dengan RF sebesar 87,8%. Skenario terbaik berdasarkan kontribusi dan peran energi tebaruk (PV-WT) adalah dari skenario ketiga dengan jumlah produksi energi lebih besar yaitu 30.691 kWh/tahun dan RF yang lebih tinggi diangka 89%.

INFO.

Info. Artikel:
No. 508
Received. September, 1, 2023
Revised. October, 12, 2023
Accepted. October, 23, 2023
Page. 829 – 840

Kata kunci:
- *Microgrid*
- *Photovoltaic*
- *Renewable Energy*
- *Renewable Fraction*
- *Wind Turbine*

Abstract

Indonesia's renewable energy mix offers an alternative to conventional fossil fuels. Indonesia has made a significant commitment to the role of exploiting this new energy in accordance with the Paris Agreement. This paper proposes the design of a microgrid architecture for a solar and wind hybrid power plant with grid-connected configuration and micro-scale power plant modeling in Ciheras Village, Cipatujah District, Tasikmalaya Regency, West Java. This architecture is divided into three scenarios in order to determine the best design qualities. The first scenario involves 50% photovoltaic (PV) and 50% wind turbine (WT), the second 60% PV and 40% WT, and the third 70% PV and 30% WT. The findings of the grid-connected microgrid were compared using supporting software, HOMER Pro. The various scenarios yielded performance analysis and renewable energy contribution. Modeling, calculation, simulation, and analysis demonstrate that the first scenario's potential energy output produces 25,655 kWh/year with an 88.2% Renewable Fraction (RF). The second scenario generates 26,194 kWh of energy per year, with a renewable fraction of 87.8%. The third scenario is the best based on the participation and role of distributed energy (PV-WT), with a higher amount of energy output of 30,691 kWh/year and a higher renewable proportion of 89%.

INTRODUCTION

With the expansion in population, the demand for electrical energy will continue to rise, as will the number of loads (industrial, residential, public facilities, etc.), hence alternative energy must become more prevalent and pursued for development[1]. The advantages of being a tropical country should benefit Indonesia in utilizing solar energy as a guarantor of future advances in photovoltaic-based technology[2].

In Indonesia, microgrid systems have not been widely used, but development is planned to produce small-medium size independent power plants and spread by utilizing power plants sourced from renewable energy and conventional power plants. In 2019, there are 75.7 million households in Indonesia, with a total power consumption of 245.5 TWh used across the archipelago[3][4]. Of course, supporting energy sources must be considered; for example, according to IRENA, the installed capacity for solar energy utilization in 2019 was 198 MW, while the capacity for wind energy utilization was 76 MW[5]. Quoted from the Ministry of Energy and Mineral Resources' website, the government strives to attain national energy independence and to increase electrification, which is not yet at 100%. The government continues to work on renewable energy (RE) development in order to meet the target of 23% RE in the national energy mix by 2025[6]. According to this remark, one strategy for reducing demand growth and increasing electrification ratio is to construct a microgrid system. It is envisaged that by constructing a microgrid system, a small-medium size independent power plant can be developed and extended by utilizing power plants derived from renewable energy and conventional plants.

A power plant in Ciheras Village, Cipatujah District, Tasikmalaya Regency, West Java, was used for microgrid modeling[7][8]. The simulation was created utilizing a hybrid plant comprised of wind energy [9] and photovoltaic-based solar energy. Some other scenarios are offered to overcome the blackout or separation of the power source from the grid, resulting in two schemes, namely on-grid and off-grid connected. Based on these possible sources, the microgrid architecture that will be used batteries serve as energy storage for the system, with the system scheme being DC/AC (DC Coupling). The HOMER Pro program was used to examine the microgrid model and test the viability of the proposed scenarios for each generating capacity. The capacity of the electrical components is predicted and tested in response to changes in the frequency of power outages from the Grid, as well as the ensuing impacts. Furthermore, the research takes into account techno-economic studies, generation performance, production, energy consumption, and contribution (%) of the two schemes, allowing the proposed optimal microgrid model to be compared and evaluated for performance. Some indications of earlier research are described in the table 1.

Table 1. Literature reviews on microgrid scenario

No	Literature	Location	Proposed Design	Tot. Power Generated
1	Shantu Ghose, et al, 2017[10].	Georgia, USA	Two scenarios of grid-connected and off-grid configuration.	PV-Inverter 25 kWp; DG 100 kW; Batt. 20 kWh; WT 10 kW.
2	Jin Shungjun, et al, 2018[11].	South Korea	Microgrid optimization model on three islands in South Korea	PV 3.1 – 4.7 kWp; WT 7500 kW; Batt. 800 – 1600 kWh.
3	Suresh Vendoti, et al, 2018[12]	Coimbatore, India	Optimization of Hybrid System for Electrification in a Rural.	PV 50 kWp; WT 3 kW; DG 100 kW; Inverter 20-60 kW.
4	Shilpa, et al, 2019[13].	Bangalore, India	Optimization of hybrid model using PV and Battery on Grid-connected.	PV 150 kWp; Batt. 100kWh; Inv. 100 kW;
5	P. Satish Kumar, et al, 2020[14].	India	Small Scale Hybrid Wind Solar Battery Based Microgrid	PV 70 W; WT 60W; and Batt. 288 Wh.
6	Quynh Tran, et al, 2021[15].	Con Dao, Vietnam	Isolation Microgrid Design for Remote Areas.	PV 60 kW; DG 40 kW, Batt 40 kWh; Inv. 40 kW.
7	Rituraj, et al, 2022[16].	Microgrid Uni. Scale	Modeling of a Microgrid System with Time Series.	PV 680 kWp; DG 50kW; and Batt. 300 kWh.
8	Handoko R, et al proposed in 2023	West Java, Indonesia	Three Scenarios On-Grid/Off-Grid Connected Systems (50%PV–50%WT), (60%PV–40%WT), and (70%PV–30%WT).	PV 14 – 19.9 kWp; WT 18 – 28.5 kW.

*PV = Photovoltaic (kWp), WT = Wind Turbine (kW), DG = Diesel Generator (kW), Inv = Inverter (kW) and Batt = Battery (kWh)

Table 1 show the microgrid system reasearch, some supporting models were created by [10], who created two scenarios of grid-connected and off-grid configuration systems with the same amount

of load. The comparison of COE values yields an economic analysis. The DC/AC microgrid model with a grid-connected system has a low COE value, indicating that the model is well optimized, with 98% renewable energy contribution to load needs. Model testing with HOMER Pro software and an economic analysis approach yielded low results when comparing the values of NPC, COE, and Operating Cost. The photovoltaic system model created includes a battery[11]. In the research by Suresh, et al[12], modeled three power systems and performed simulated optimization using system data from isolated South Korean islands. Microgrid optimization analysis was performed in the Indian state of Karnataka, in the Chamarajanagar area of Indiganatha Village. Because the intended location is not connected to the main power grid, the proposed system is off-grid. Wind turbines, solar panels, and diesel generators (conventional generation) are used to power the hybrid generation model. Because the community is not connected to the main grid, this generation model must be studied and optimized. Shilpa et al. offer a campus-based on-grid rooftop PV system with an appropriate battery bank as a backup power source in Bangalore, India[13]. Another study described the feasibility study of a microgrid model, which was put to the test in a variety of situations with diverse architectural designs. The main grid, generator sets, and electrical loads make up the first scenario, whereas the main grid, generator sets, electrical loads, wind turbines, batteries, and inverters make up the second[14][15]. Software was used to test and analyze the microgrid model while keeping track of factors including COE, NPC, energy generation, and renewable portion. According to the simulation results, the second scenario microgrid model has a lower COE value and is more cost-effective than the first scenario microgrid model[16].

The goals of this paper include modeling and calculating the generation capacity of solar and wind energy on grid-connected microgrids without utilizing Homer Pro 3.11.2 software based on simulated scenarios. Then, examine the impact of power failures on the microgrid and the variation in average repair time on the microgrid model. Furthermore, evaluate and contrast the three offered scenarios, as well as the gain in solar and wind energy output throughout a year. In addition to examining the renewable fraction gain and economic analysis (COE and starting capital), the proposed microgrid model is evaluated and recommended based on the performance and economic findings of the three scenarios and configurations employed.

This paper consists of four Section, the introduction section contains background, microgrid design problems, and references related to the research, section two contains relevant research methods and modeling, section three contains a discussion of the results of testing the capacity of microgrid electrical components and techno-economic analysis, and section four concludes with conclusions and results that correspond to the research objectives.

RESEARCH METHOD

Microgrid modeling and analysis is located at 7.738112751361012° south latitude, 107.97030760296646° east longitude, and 14 meters above sea level. The average wind speed at this area is 3-4 m/s, with a maximum speed of 12 m/s. The average wind speed in a one-year time interval based on data from the previous three years in a 12-month period is 3.83 m/s. The highest wind speed recorded was 5.00 m/s in July, and the lowest wind speed recorded was 2.50 m/s in April 2020. The average value of the Global Horizontal Irradiation (GHI) over a year is 4.75 kWh/m^2/day, with September having the highest value at 5.54 kWh/m^2/day and January having the lowest value at 4.01 kWh/m^2/day. Because 1 PSH equals 1 kWh/m^2/day, the GHI value becomes a parameter in establishing the Peak Sun Hour (PSH). Currently, the average annual value is 27.7°C.

The same design microgrid model is simulated in three scenarios, with the energy demand in one day divided into two halves, the first of which is covered by PV and the second by WT. Variations are done to acquire the ideal model by increasing the capacity of one plant and decreasing the capacity of another plant, so that the initial condition of the scenario is 50% PV capacity and 50% WT capacity. Variations were made in this investigation with a vulnerability of 50% (first scenario), 60% (2nd scenario), and 70% (3rd scenario).

Figure 1. Microgrid location and site modeling

Table 2. Existing domestic load

Categori	Power (kW)	Daya (kVA)	Energy (kWh/hari)	Energy (kVAh/hari)
Component	6.64	7.64	28.31	32.54
Lighting	0.44	0.50	5.24	6.03

Table 3. Energy demand and component is used to determine generation capacity scenarios

Scenario	Percentage (%)		Tot. Capacity (kW)			Tot. Quantity (pcs)			
	PV	WT	PV	WT	Inv	PV	WT	SCC	WTCC
1	50	50	14.061	19,000	26100	43	39	5	19
2	60	40	17.004	15,000	22200	52	31	5	15
3	70	30	19.947	12,000	22300	61	23	7	12

Table 4. Microgrid electrical simulation data specifications

Component	Rated Power/Capacity	Information	Life Design (Years)
PV Panel	327 Wp	SunPower, Mono-crystalline.	25
Wind Turbine	1000 W	A-Wing, Horizontal Axis WT.	20
Battery	205 Ah	Trojan, VRLA AGM.	5
Inverter	A:8000/B:5000W DC Power	SolaX Power, MPPT Full	25
SCC	9000 W	Morning Star, MPPT (η 97.9%).	15
WTCC	1500 W	A-Wing International.	15

Direct observation was carried out, as well as activities to record power demands for the lighting category, daily energy consumption, sun irradiation data, and wind speed gathered as secondary data using meteonorm 8 software. Table 2 depicts the household load at the proposed site location, where the equipment load includes electronic equipment load and lighting load in a single day. According to preliminary research and simulations, the production that can be created is 3,876 kWh/year, with an energy consumption of 12,251 kWh/year; however, existing microgrid capacity cannot match the load requirements, and RE plants can only cover 3.16% of energy needs in one day.

The increase is limited to 70% to prevent one of the plants from dominating and overcoming the intermittent nature of the other plants. The model is tested using simulations with 50%, 60%, 70%, and 80% capacity vulnerabilities based on energy demand in one day to assure which plants will increase and reduce their capacity. Energy production comparison of PV and WT when simulated from 50% to 80% capacity based on energy consumption in one day. Because the energy production of PV is more than that of WT, with an average difference of 14,007 kWh/year, the capacity of PV will be increased and the capacity of WT will be decreased, as shown in Table 3.

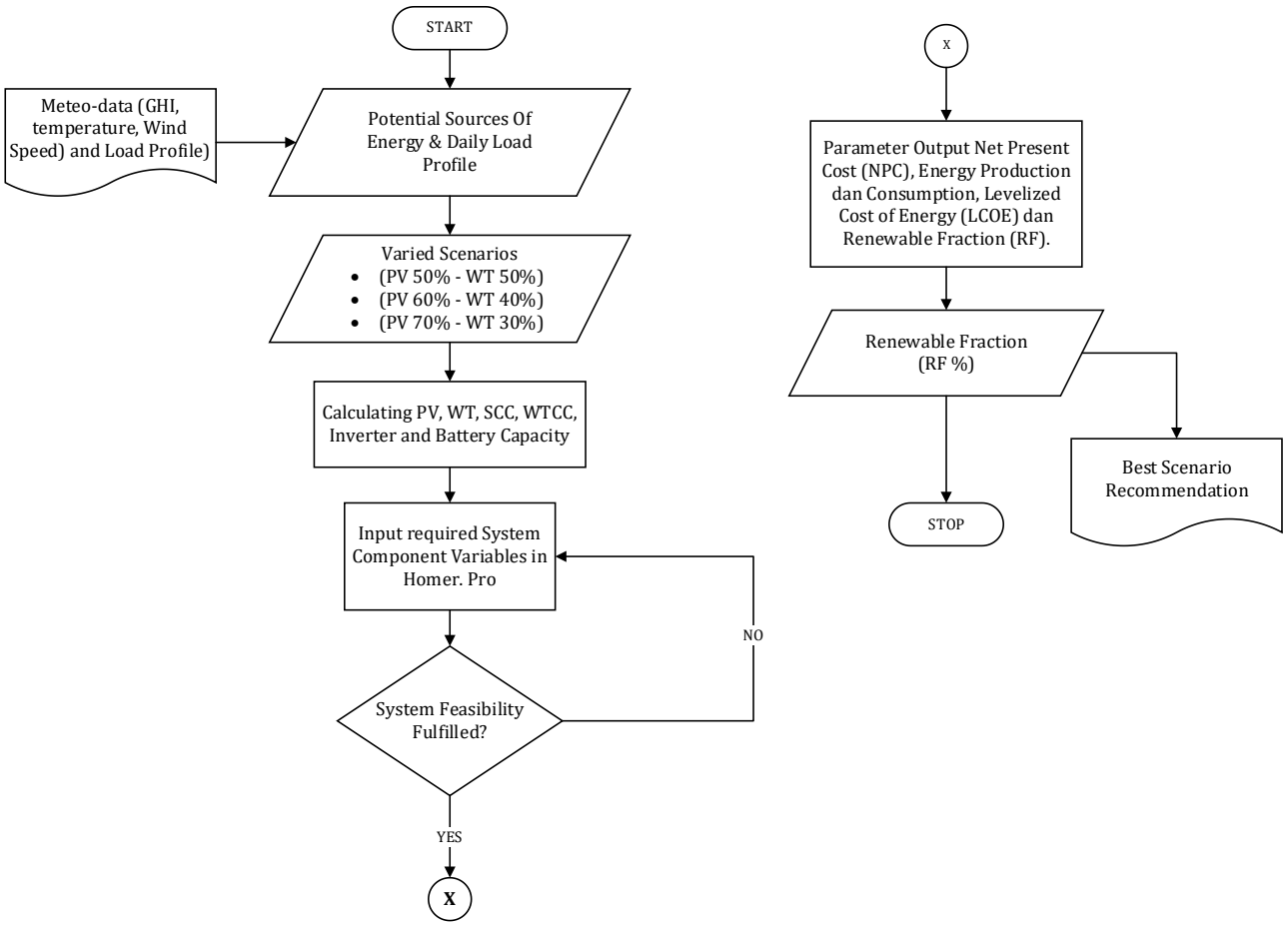

Figure 2. Modeling and simulation method

To carry out its capacity role, the microgrid system is made up of many electrical components. Table 4 shows the simulation parameters for the selected microgrid electrical components and their specifications. Microgrid electrical components are designed to work with the microgrid architecture, which includes generating units (PV panels and wind turbines), energy storage, power backup, power conversion, and the Grid. The Directorate General of New Renewable Energy and Energy Conservation's reference for the selection of electrical components is considered and chosen[17][18]. Because the grid is unlike any other Component, HOMER Pro calculates grid costs in a unique method[19]. The grid cost output computation is divided into the grid capital cost and the grid operating cost. If the system is linked to the grid and includes other power-generating devices (such as microturbines, fuel cells, PV arrays, or wind turbines), the grid capital cost equals the connectivity cost. Otherwise, the capital cost of the grid is nil. Each microgrid electrical component's price must be known and entered into the HOMER Pro software program.

The proposed simulation in Figure 2 then proceeds to the following step, which consists of three possibilities based on the energy demand in one day. The microgrid electrical components are determined for each scenario based on the results of calculations and visual descriptions to determine the capacity of the SCC. After determining the capacity of the microgrid electrical components and comparing them to the datasheet specifications, the next component variable in HOMER Pro is filled. The model is then calculated using HOMER Pro software, and if there are no problems where there is a feasible statement, the results of economic data and microgrid performance are assessed. If the computation results contain infeasible information, the component variable filling is repeated until the calculation results become feasible. Once the data parameters are established, the generating capacity of each renewable energy plant may be calculated based on the load profile and natural energy potential at the research site.

Solar panel requirements are calculated based on AS/NZS 4509.1 standard, 2009[20][21] based on the known load profile. The temperature factor (f_{temp}) is calculated based on equation (1) and the effective cell temperature ($T_{cell_{eff}}$) is calculated based on equation (2). Equation (3) is used to determine the output power of the module affected by the derating factor. From the calculation results, the value of the effective cell temperature ($T_{cell_{eff}}$) is 52.7°C while the value of the temperature factor (f_{temp}) is 0.89 and the value of the derating factor due to dust f_{dirt}) is 1, the value is obtained from table 2.3 when the solar panel is in a clean condition and the value of the manufacturing derating factor (f_{man}) is 0.9. From these three variables that become derating factors, the module output power value (P_{mod}) is 261.92 Wp using equation (3).

$$N = \frac{(E_d \times f_o)}{P_{mod}.G.\eta_{PVSS}} \quad (1)$$

$$f_{temp} = 1 - \gamma(T_{cell_{eff}} - T_{STC}) \quad (2)$$

$$P_{mod} = P_{STC}.f_{man}.f_{temp}.f_{dirt} \quad (3)$$

Wind turbine capacity is calculated using equation (4) based on the characteristics of wind speed to wind turbine output power. Where the wind turbine's nominal power value is determined using equation (5) or derived from the product datasheet in the wind speed to power curve section. The power factor of the electrical system is considered to be 0.87. The simulation is divided into three scenarios, each with a percentage of generation capacity based on daily energy demand.

$$N = \frac{Ed}{Pnom} \quad (4)$$

$$P = \left(C_p \varepsilon_g \varepsilon_b\right) \frac{1}{2} \rho_a A_T v^3 \quad (5)$$

Equation (4) represents a simple equation used to determine the number or capacity of required wind turbines, where the nominal power value (Pnom) is calculated from equation (5) under average manufacturing speed conditions. Although wind turbines have the same capacity, for example, 500 watts, the wind speed for cut-in and cut-off varies based on the wind turbine characteristics. The wind turbine datasheet includes a wind Power-Speed curve that depicts the wind turbine's characteristics. The battery capacity is determined based on the AS/NZS 4509.2 standard in 2010[22], from the calculation results using equation (6), the battery capacity is 5,503.12 Ah with an autonomous time value (T_aut) for three days, the maximum depth of discharge value (DoD_max) of 0.8, and the total energy required (E_tot) based on energy needs at night of 17,610 Wh. The battery capacity figure is divided by the nominal capacity of the used battery, yielding a total of 25 batteries.

$$C_{x\_Ah} = \frac{E_{tot}}{V_{DC}} \times \frac{T_{aut}}{DoD_{maks}} \quad (6)$$

The value of C_X is the battery capacity when discharged with a specific value (x) in units of (Ah), E_{tot} is the total energy required (Wh), T_{aut} is the number of autonomous days, V_{DC} is the nominal battery voltage (V), and DoD_{maks} is the maximum discharge capacity of the battery, as shown on the datasheet. Due to the nominal voltage of the battery of 12 V and the nominal voltage of the DC bus of 24 V, the battery must be given in such a way that the number of batteries required was multiplied by 2, yielding a total of 50 batteries. The battery is used as the primary power backup system that can fulfill the needs of the load when the power supplied by the generator from renewable energy is low, thus its capacity must be carefully calculated to ensure the stability of the microgrid system.

Table 5. Energy production and consumption data (On-grid)

Scenario	Production (kWh/yr)		Consumption (kWh/yr)
	Photovoltaic	Wind Turbine	AC Main Load
1	18,581	7,072	12,251
2	20,611	5,583	12,251
3	26,224	4,467	12,251

Table 6. Energy production and consumption data (Off-grid)

Scenario	Production (kWh/yr)		Consumption (kWh/yr)		Quantity (kWh/yr)
	Photovoltaic	Wind Turbine	AC Main Load	Losses	Excess Electricity
1	18,583	7,072	12,251	991	12.369
2	20,611	5,583	12,251	1,023	12,876
3	26,224	4,467	12,251	1,053	17,343

Table 7. Energy production and consumption in Average time of Power Outage (1st Scenario)

Average time of power outage (Hour)	Production (kWh/yr)	Consumption (kWh/yr)		Quantity (kWh/yr)
	Purchased Energy	Energy for Sale	Losses	Excess Electricity
2	3,335	15,911	773	6.14
4	3,326	15,872	774	32.1
6	3,319	15,813	773	84,4
8	3,321	15,724	770	178
10	3,307	15,657	772	231
12	3,294	15,594	772	281
14	3,281	15,596	775	264

Table 8. Energy production and consumption in Average time of Power Outage (2nd Scenario)

Average time of power outage (Hour)	Production (kWh/yr)	Consumption (kWh/yr)		Quantity (kWh/yr)
	Purchased Energy	Energy for Sale	Losses	Excess Electricity
2	3,513	16,612	789	6.0
4	3,502	16,573	790	30.0
6	3,495	16,509	790	86.8
8	3,497	16,416	786	185
10	3,482	16,344	788	241
12	3,469	16,281	788	292
14	3,456	16,283	792	275

Table 9. Energy production and consumption in Average time of Power Outage (3rd Scenario)

Average time of power outage (Hour)	Production (kWh/yr)	Consumption (kWh/yr)		Quantity (kWh/yr)
	Purchased Energy	Energy for Sale	Losses	Excess Electricity
2	3,675	21,117	924	21.8
4	3,664	21,070	925	56.2
6	3,657	20,988	924	131
8	3,658	20,876	920	248
10	3,642	20,786	921	322
12	3,629	20,701	921	396
14	3,616	20,699	923	384

The Solar Charge Controller's capacity is decided by a scenario that is divided into three different situations. The first scenario (PV 50%; WT 50%) used 43 solar panels, with each solar panel constructed in series and parallel to produce the V_{OC} and I_{SC} values of the PV array according to the SCC.

In the first scenario, the number of solar panel strings linked to the combiner box is eight, with each PV module string consisting of five series-connected PV modules with the same PV module specs.

One string of three series-connected PV modules is used in combiner box number five. Because each PV array arrangement meets the SCC capacity, each PV array has the same SCC criteria. According to the number of PV panels given in Table 3, the number of SCCs in the second and third scenarios is 5 and 7, respectively. In terms of WTCC capacity based on the number of wind turbines used, for scenario 1, the number of wind turbines utilized in the first scenario is 39, hence the number of WTCCs is 19. The number of wind turbines used in the first scenario is 31, hence the number of WTCCs is the same as 15 in the second scenario. The third possibility Because there are 23 wind turbines in the first scenario, there are 12 WTCCs. The first scenario had the highest maximum inverter output power of 26.1 kW, while the second scenario had the lowest maximum inverter output power of 22.2 kW - 22.3 kW. When the calculation results are compared to the simulation results, three to five inverters are required for each scenario, depending on the kW size chosen.

RESULTS AND DISCUSSION

The simulation outputs are microgrid performance data, which include microgrid energy production and consumption, energy production from the proposed PV and WT systems, and renewable energy contribution expressed as a renewable fraction (%). Furthermore, the simulation results are presented in the form of a techno-economy for a 25-year design.

Microgrid Energy Production and Consumption

Table 5 – Table 6 displays the results of the first, second, and third simulation situations. Purchased energy fluctuates; a 2 kWh/year rise happens when the average time condition of power interruptions is at 8 hours. Meanwhile, when the average duration of power outages is longer than 8 hours, the cost of purchased energy rises. The energy sold fluctuates similarly to the purchased energy; when the average time circumstances of power outages are between 2 and 12 hours, the energy sold increases. Meanwhile, when the average duration of power outages is 14 hours, the amount of energy sold increases by 2 kWh each year. Variations in the price of energy sold and purchased as a result of the frequency of grid power outages and the average repair time. When there are power outages and repair times, the net metering export and import procedure is impeded. As a result, the energy generated by PV and WT cannot be exported to the grid. When the energy generated by PV and WT is low, the Grid energy import process is hampered. When the typical grid outage time conditions are 2 to 12 hours, the value of excess electricity in the grid-connected microgrid model increases; when conditions are 14 hours, excess electricity falls by 17 kWh per year. Because the microgrid model is not connected to the network, the value of extra electricity does not change in the event of grid power disruptions. As a result, the excess electricity value of 12,425 kWh per year goes underutilized (not exported to the grid or stored in the battery).

The dispatch is defined by the power flow due to the simulation's usage of a load flow controller. Excess electricity happens when the energy generated by PV and WT exceeds the load capacity and the energy in the battery is depleted, resulting in the energy not being used. Another cause is a grid outage, which means that more energy cannot be transmitted to the grid, resulting in excess electricity. Energy bought and sold fluctuated similarly to the first scenario, with energy purchased increasing by 2 kWh per year when the average grid outage time condition was 8 hours. Purchased energy has decreased in addition to the 8-hour condition. Energy sold increased by 2 kWh per year when the average time circumstances of grid outages were in the 14-hour condition. Aside from the 14-hour constraint, the amount of energy sold reduced. It can be shown that the change in the value of excess electricity in the grid-connected microgrid model has reduced by 17 kWh/year when the average grid outage period is 14 hours; otherwise, excess electricity has increased.

Tables 7–9 show the energy output and consumption of the grid-connected microgrid model in each of the three scenarios. Changes fluctuate in the first, second, and third scenarios when energy is bought and sold. When the average grid outage period is 8 hours, the purchased energy increases by 1 kWh/year; otherwise, the sold energy increases. In terms of energy sold, it grew in all conditions of average time of grid disruptions. Energy sales increased when compared to the first, second, and third scenarios. Whereas energy sold climbed by an average of 2,826 kWh/year from the first to the second

scenario, energy sold increased by 2,327 kWh/year from the second to the third scenario. This occurred as a result of an increase in PV and WT energy production, which resulted in an increase in energy sold. Meanwhile, the offgrid scheme simulation results tend to have the same production and energy consumption numbers (see Tables 5 and 6).

The value of excess electricity in the grid-connected microgrid model declined by 12 kWh/year when the average time of power outage by the Grid was at 14 hours, but climbed when the average time of power outage by the Grid was at 14 hours. When the value of surplus electricity is compared between the first, second, and third scenario simulations. The first scenario simulation's average excess electricity value of 154 kWh/year is lower than the second and third simulation scenarios' notional excess electricity values of 159 kWh/year and 222.7 kWh/year.

Renewable Fraction (PV and WT)

Following the description of the simulation findings for microgrid energy generation and consumption. As part of the study of all scenarios, a comparison of renewable energy output with grid-connected and offgrid microgrid designs is performed. The contrast is depicted in Figure 3. The graph depicts the energy output of PV and WT, as well as the total energy produced by both in the first, second, and third simulated scenarios. Due to an increase in PV capacity and a drop in WT capacity, PV energy output grew by 2,028 kWh/year from the first scenario to the second scenario, while WT energy production declined by 1,489 kWh/year. The next scenario (beginning with the first scenario) will see an increase in total renewable energy output based on the ratio of energy increase and decline. PV energy production showed an increase of 7,641 kWh/year from the first scenario to the third scenario while WT energy production decreased by 2,605 kWh/year from the first scenario to the second scenario. The increase in PV energy production and the decrease in WT production were adjusted to 5,036 kWh/year, from this value, the total renewable energy production from the first scenario to the third scenario increased by 5,036 kWh/year. Renewable fraction is a metric used to calculate renewable energy generation's contribution to fulfilling load requirements. The software calculates the renewable fraction, which is shown in Table 10. The renewable fraction value varies depending on the scenario. The renewable fraction is impacted by purchased energy, sold energy, and AC load energy in the simulation.

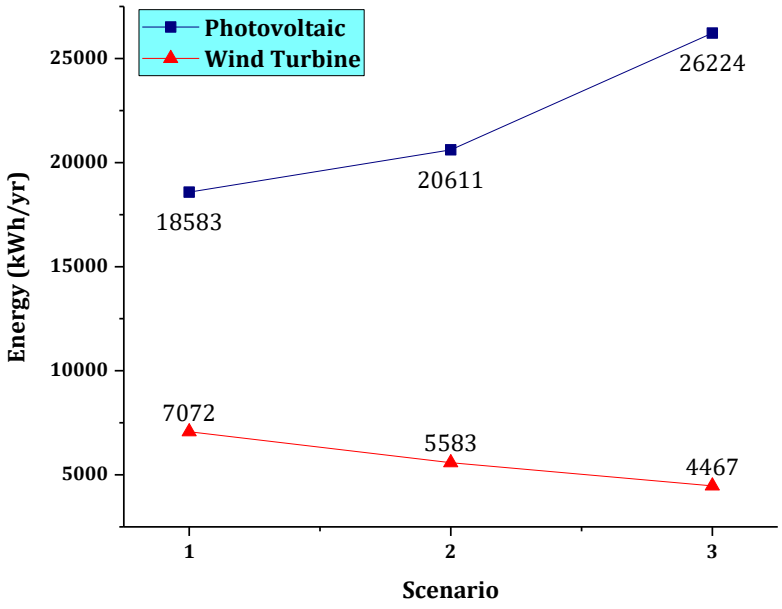

Figure 3. Renewable Energy Production (PV and WT)

Table 10. Renewable Fraction On-grid and Off-grid using Average Time of Power Outages

Average time of power outage (Hour)	Renewable Fraction (%)					
	On-grid Scenario			Off-grid Scenario		
	1st	2nd	3rd	1st	2nd	3rd
2	87.8	88.2	89	100	100	100
4	87.8	88.2	89	100	100	100
6	86.8	88.2	89	100	100	100
8	87.8	88.2	89	100	100	100
10	87.8	88.1	89	100	100	100
12	87.8	88.2	89	100	100	100
14	87.9	88.2	89	100	100	100

Because the nominal AC load energy is fixed in all situations, the change in the value of purchased and sold energy determines the nominal renewable fraction. In this scenario, the grid-connected microgrid model clearly shows the relationship between the nominal renewable fraction and grid failures, which result in fluctuating changes in energy sold and purchased. Given the prior energy output and consumption, the nominal renewable fraction in all simulated scenarios for the off-grid microgrid is 100%. This chart compares energy production to consumption; energy production is in surplus. According to Table 6 in the first scenario simulation, PV and WT energy output totaled 25,655 kWh/year, while energy consumption totaled 13,242 kW/year, resulting in 12,369 kWh/year of unused power (excess electricity).

CONCLUSIONS

The following findings were reached based on simulation results and analysis of grid-connected and off-grid microgrid models. Based on the calculation results for the first scenario, microgrid modeling necessitates PV and WT capacity of 14.061 kW and 19 kW. The second case involves 17.004 kW and 15 kW. The third case involves 19.947 kW and 12 kW. The findings of the microgrid simulation reveal that the frequency of power outages and the time it takes to repair them cause fluctuating changes in the buying and selling of energy on the distribution network side. When the average time of power outage by the grid is 2-12 hours, the process of extra electricity grows by 55 kWh/year for the first scenario, 57 kWh/year for the second scenario, and 75 kWh/year for the third scenario. While in the 14-hour condition, it reduced by 17 kWh/year for the first and second scenarios and 12 kWh/year for the third. PV energy production grew by 2,028 kWh/year between the first and second scenarios, and by 7,641 kWh/year between the second and third scenarios. Meanwhile, WT energy dropped by 1,489 kWh/year between the first and second scenarios, and by 1,116 kWh/year between the second and third scenarios. However, from the first to the third scenario, total PV and WT energy production increased by 5,036 kWh/year. According to the research results, the third scenario with 70% PV capacity and 30% WT has the highest overall renewable energy generation of 30,691 kWh/year. While the first scenario has the lowest overall renewable energy output with a nominal value of 25,655 kWh/year. According to the results of the grid-connected microgrid performance research, the third scenario has the greatest average renewable fraction value of 89.0%. While the second scenario has the lowest average renewable portion value of 87.6%. The three scenarios on the off-grid microgrid have a renewable proportion of 100%, indicating that they can meet the load requirements.

ACKNOWLEDGMENTS

The authors would like to thank PT Lentera Bumi Nusantara for the opportunity to survey and collect data in the initial feasibility study in 2021, as well as the team involved in the research at Universitas Jenderal Achmad Yani's Electrical Engineering Laboratory.

REFERENCE

[1] H. Wirawan and Y. M. L. Gultom, "The effects of renewable energy-based village grid electrification on poverty reduction in remote areas: The case of Indonesia," *Energy Sustain. Dev.*, vol. 62, pp. 186–194, 2021,

doi: 10.1016/j.esd.2021.04.006.

[2] M. S. Islami, T. Urmee, and I. N. S. Kumara, "Developing a framework to increase solar photovoltaic microgrid penetration in the tropical region: A case study in Indonesia," *Sustain. Energy Technol. Assessments*, vol. 47, no. June, p. 101311, 2021, doi: 10.1016/j.seta.2021.101311.

[3] D. Simatupang *et al.*, "Remote Microgrids for Energy Access in Indonesia—Part I: Scaling and Sustainability Challenges and A Technology Outlook," *Energies*, vol. 14, no. 21, pp. 1–23, 2021, doi: 10.3390/en14216901.

[4] D. Simatupang *et al.*, "Remote Microgrids for Energy Access in Indonesia—Part II: PV Microgrids and a Technology Outlook," *Energies*, vol. 14, no. 21, pp. 1–18, 2021, doi: 10.3390/en14216901.

[5] IRENA, *International Renewable Energy Agency*, 2020th ed. Abu Dhabi: IRENA, 2020.

[6] "Direktorat Jenderal EBTKE - Kementerian ESDM." https://ebtke.esdm.go.id/post/2019/10/17/2369/berikut.strategi.pemerintah.dalam.pengembangan.ebt.menuju.kemandirian.energi.nasional (accessed Jun. 04, 2023).

[7] M. Abdillah, T. Mutia, T. A. Nugroho, and N. I. Pertiwi, "Design of Automatic Transfer Switch on A Renewable Energy Hybrid Grid System at PT Lentera Bumi Nusantara," *J. Adv. Technol. Multidiscip.*, vol. 1, no. 2, pp. 38–44, 2022, doi: 10.20473/jatm.v1i2.40293.

[8] R. Simatupang and D. Supriatna, "Designing a Tapperless Blade with an S-4320 Airfoil on a Micro-Scale Horizontal Axis Wind Turbine (Case Studies at PT Lentera Bumi Nusantara)," *J. Mech. Electr. Ind. Eng.*, vol. 3, no. 1, pp. 27–34, 2021, doi: https://doi.org/10.46574/motivection.v3i1.81 Designing.

[9] A. Nuraini, C. Slamet Abadi, and D. Fachruddin, "Analisis Perbandingan Bilah Turbin Angin Jenis Taper dengan Taperless pada Turbin Angin Skala Mikro di PT. Lentera Bumi Nusantara," in *Prosiding Seminar Nasional Teknik Mesin Politeknik Negeri Jakarta*, 2019, pp. 138–146, [Online]. Available: https://prosiding-old.pnj.ac.id/index.php/sntm/article/view/2011.

[10] S. Ghose, A. El Shahat, and R. J. Haddad, "Wind-solar hybrid power system cost analysis using HOMER for Statesboro, Georgia," in *Conference Proceedings - IEEE SOUTHEASTCON*, 2017, pp. 3–6, doi: 10.1109/SECON.2017.7925324.

[11] S. Jin, H. Kim, T. H. Kim, H. Shin, K. Kwag, and W. Kim, "A Study on Designing Off-grid System Using HOMER Pro - A Case Study," in *IEEE International Conference on Industrial Engineering and Engineering Management*, 2019, pp. 1851–1855, doi: 10.1109/IEEM.2018.8607423.

[12] S. Vendoti, M. Muralidhar, and R. Kiranmayi, "HOMER Based Optimization of Solar-Wind-Diesel Hybrid System for Electrification in a Rural Village," in *2018 International Conference on Computer Communication and Informatics, ICCCI 2018*, 2018, pp. 1–6, doi: 10.1109/ICCCI.2018.8441517.

[13] S. Shilpa and H. Sridevi, "Optimum design of Rooftop PV System for An Education Campus Using HOMER," Oct. 2019, doi: 10.1109/GCAT47503.2019.8978446.

[14] P. S. Kumar, R. P. S. Chandrasena, V. Ramu, G. N. Srinivas, and K. V. S. M. Babu, "Energy Management System for Small Scale Hybrid Wind Solar Battery Based Microgrid," *IEEE Access*, vol. 8, pp. 8336–8345, 2020, doi: 10.1109/ACCESS.2020.2964052.

[15] Q. T. Tran, K. Davies, and S. Sepasi, "Isolation Microgrid Design for Remote Areas with the Integration of Renewable Energy: A Case Study of Con Dao Island in Vietnam," *Clean Technol.*, vol. 3, no. 4, pp. 804–820, 2021, doi: 10.3390/cleantechnol3040047.

[16] R. Rituraj, S. Ali, and A. R. V. Koczy, "Modeling of a Microgrid System with Time Series Analysis using HOMER Grid Software and it's Prediction using SARIMA Method," *Robot Autom Eng. J.*, vol. 5, no. 2, pp. 1–21, 2022, doi: 10.19080/RAEJ.2022.05.555660.

[17] Directorate-General for New Renewable Energy and Energy Conservation, "Clean Energy Development Collaboration to Support the One Million Solar Roof and Green Airport Movement," Jakarta, 2020. [Online]. Available: https://ebtke.esdm.go.id/post/2020/09/26/2637/kolaborasi.pengembangan.energi.bersih.dukung.gerakan.sejuta.surya.atap.dan.green.airport.

[18] Directorate-General for New Renewable Energy and Energy Conservation, "Accelerating Rooftop PV, the Ministry of Energy and Mineral Resources Prepares the Nusantara Energy Program," Jakarta, 2020. [Online]. Available: https://ebtke.esdm.go.id/post/2020/09/26/2636/akselerasi.plts.atap.kementerian.esdm.siapkan.program.energi.surya.nusantara.

[19] S. Syafii, P. Anugrah, H. D. Laksono, and H. Yamashika, "Economic Feasibility Study on PV/Wind Hybrid Microgrids for Indonesia Remote Island Application," *TEM J.*, vol. 10, no. 4, pp. 2001–2006, 2021, doi: 10.18421/TEM104-66.

[20] AS/NZS 4509.1, "Australian / New Zealand Standard ™ Stand-alone power systems Part 1 : Safety and installation," *1*. p. 8, 2009.

[21] H. R. Iskandar, N. Heryana, N. Winanti, G. A. Setia, R. Ridwanulloh, and M. R. Alfarizi, "Optimal Design of

Rooftop PV Systems for Electrical Engineering Department Laboratory," in *2021 3rd International Conference on High Voltage Engineering and Power Systems, ICHVEPS 2021*, 2021, pp. 349–354, doi: 10.1109/ICHVEPS53178.2021.9601097.

[22] AS/NZ 4509.2:2010, "Stand-alone Power System," in *Australian/New Zealand Standard. Part -2 System Design System Design*, 2nd ed., Wellington: SAI Global Limited, 2010, pp. 1–112.